Volume Title
*ASP Conference Series, Vol. **Volume Number***
Author
*© **Copyright Year** Astronomical Society of the Pacific*

Probing High-Column Outflows in BALQSOs Using Metastable Helium

Karen M. Leighly,[1] Adrian B. Lucy,[1] Matthias Dietrich,[2] Donald Terndrup,[2,3] and Sarah C. Gallagher[4]

[1]*Homer L. Dodge Department of Physics and Astronomy, The University of Oklahoma, 440 W. Brooks St., Norman, OK 73019,* [2]*Department of Astronomy, The Ohio State University, 4055 McPherson Lab, 140 W. 18th Ave, Columbus, OH 43210,* [3]*National Science Foundation, 4201 Wilson Blvd., Arlington, VA 22230,* [4]*Department of Physics and Astronomy, The University of Western Ontario, 1151 Richmond Street, London, ON N6A 3K7, Canada*

Abstract. Outflows are believed to be ubiquitous and fundamentally important in active galaxies. Despite their importance, key physical properties of outflows remain poorly unconstrained; this severely limits study of the acceleration process. It is especially difficult to constrain the column density since most of the lines are saturated. However, column densities can be measured using ions that are expected to be relatively rare in the gas, since they are least likely to be saturated. Phosphorus, specifically the P v doublet at 1118 and 1128Å, is generally regarded as a useful probe of high column densities because of its low abundance. We have found that the metastable neutral helium triplet is an equally valuable probe of high column densities in BALQSOs. The significant advantage is that it can be observed in the infrared (He i*λ10830) and the optical (He i*λ3888) bands from the ground in low-redshift ($z < 1.2$) objects.

We report the discovery of the first He i*λ10830 BALQSO FBQS J1151+3822, and discuss constraints on the column density obtained from the optical and IR He i* lines. In addition, a new observation revealing Mg ii and Fe ii absorption provides further constraints, and *Cloudy* modeling of He i*, Mg ii and Fe ii suggests that the difference between LoBALs and FeLoBALs is column density along the line of sight.

1. The Remarkable Properties of He i*

Neutral helium has interesting atomic structure that makes it a useful astrophysical tool. The 2s level of the triplet state is metastable with a lifetime of 2.2 hours, and it acts as a second ground state. The 2s level lies 19.75 eV above the ground state, so it is populated by recombination. It is depopulated predominantly by collisions in photoionized gas. This means that He i* absorption measures the He^{+} column, and He i* absorption occurs along with other high-ionization absorption lines including C iv, Si iv, and P v.

It has been known for $\sim$15 years that many quasar absorption lines are saturated but not black because the absorber only partially covers the continuum source (e.g., Hamann 1998). So, to estimate column densities, one needs absorption lines that are not easily saturated, i.e., from rare ions. Then, two or more transitions from the same lower level have ratios fixed by atomic physics, and measurements of optical depths of lines from such transitions can be used to solve for the covering fraction. Phosphorus

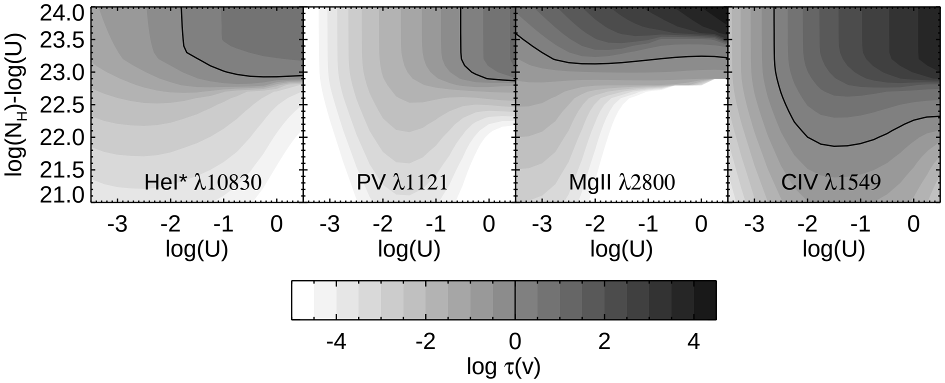

Figure 1. Predicted opacity contours for a square absorption line with a width of 10,000 km s^{-1}. He ɪ*λ10830 has nearly the same opacity as P ᴠ over a broad area of parameter space. In contrast, at high values of $\log(N_H) - \log(U)$, lines from common ions such as C ɪᴠλ1549 would be saturated.

is a low-abundance element (765 times less abundant than carbon). The P ᴠ resonance doublet at 1118 and 1128Å is a good probe of high-column outflows (Hamann 1998).

Although helium is abundant in astronomical gas, He ɪ* is rare. One of every ~175,000 He^+ atoms is He ɪ* in a typical plasma (Clegg 1987). The He ɪ*λ10830 (2s→2p) and He ɪ*λ3889 (2s→3p) lines are suitable for measuring the He^+ covering fraction and column density. As shown in Fig. 1, He ɪ* has very similar opacity as P ᴠ. But He ɪ* has the added advantage that it is observable from the ground in the optical and IR in low redshift objects.

He ɪ* has another important advantage over other lines. A line's opacity is proportional to λf_{ik}, where f_{ik} is the oscillator strength. So the optical depth ratio of two transitions from the same level is equal to the λf_{ik} ratio. This ratio is ~2 for hydrogen-like resonance doublets (including P ᴠ). In contrast, the ratio of λf_{ik} for He ɪ*λ10830 to He ɪ*λ3889 is 23.3. This means that these two lines provide a large dynamic range for measuring the spatially-averaged optical depth. Specifically, He ɪ*λ10830 is sensitive to lower column densities, and He ɪ*λ3889 takes over at higher column densities. Simulations show that the average column density can be accurately recovered over almost 2.5 orders of magnitude (Leighly et al. 2011, Fig. 19).

2. FBQS J1151+3822: The First He ɪ*λ10830 BALQSO

We observed FBQS J1151+3822 (z=0.3344, $m_v = 15.7$, $M_V = -25.6$) in March 2008 using SpeX on the NASA Infrared Telescope Facility (IRTF) as part of another project. We serendipitously discovered a prominent broad absorption feature that could only be attributed to He ɪ*λ10830. While absorption from He ɪ*λ3889 has been observed in other objects, this was the first report of a broad absorption line in He ɪ*λ10830. This work is described in Leighly et al. (2011).

Absorption from He ɪ* at 3889Å is not obvious in FBQS J1151+3822 because of strong Fe ɪɪ emission. However, the 3889Å component could be recovered using an Fe ɪɪ template model. The ratio of the data to continuum is shown for the He ɪ*λ10830 and He ɪ*λ3889 lines in Fig. 2. We used standard partial covering analysis (e.g.,

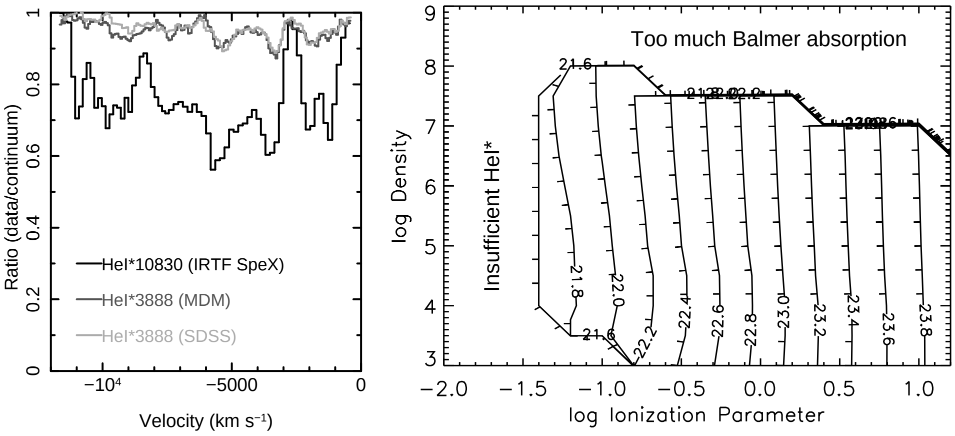

Figure 2. *Left:* The ratio of data to continuum as a function of velocity for the He I* lines in FBQS J1151+3822. *Right:* Contours of the total log hydrogen column density [cm^{-2}] required to produce the measured average He I* plotted as a function of the log of the ionization parameter U and the log of the hydrogen density [cm^{-3}]. See Leighly et al. (2011) for details.

Hamann et al. 1997; Arav et al. 2005) to derive the optical depth and covering fraction as a function of velocity. Integration over the optical depth yields a log He I* column density of ~15.6 [cm^{-2}]. The spatially-averaged log column density (i.e., $C_f\tau$, where C_f is the covering fraction, e.g., Arav et al. 2005) is ~14.9. There are no Balmer absorption lines in the spectrum, so we obtain an upper limit on hydrogen in the $n = 2$ level.

Cloudy modeling was used to determine the total hydrogen column density, where solar abundances were assumed throughout. We show in Fig. 2 the contours of total hydrogen column density required to produce the observed average He I* column density. Low ionization parameters produce insufficient He I* because the He^{+} region is too thin. High densities violate the Balmer absorption upper limit. The column densities estimated for FBQS J1151+3822 are comparable to or larger than those from several objects presented by Dunn et al. (2010) (also obtained using partial covering analysis). This demonstrates the sensitivity of He I* to high column densities.

3. Mg II and Fe II Absorption in FBQS J1151+3822

We observed FBQS J1151+3822 in May 2011 at the KPNO 4-meter telescope using the RC spectrograph. We detected, for the first time, a broad absorption feature shortward of the Mg II emission line (Fig. 3; Lucy et al. in prep.).

Clearly, Mg II absorption is present in the spectrum. We conclude that absorption from Fe II and excited state Fe II is also present. We construct absorption profiles for Mg II and Fe II using the He I*λ10830 profile, thereby assuming that all of these lines are produced in the same gas (the justification for this assumption will be discussed in Lucy et al. in prep.). The Fe II divides nicely into ground state and low ionization lines ($\lambda < 2600$Å), and higher ionization lines (2600–2750Å). We fit the spectrum with these profiles (Fig. 3). Integrating over the resulting apparent optical depths yields apparent

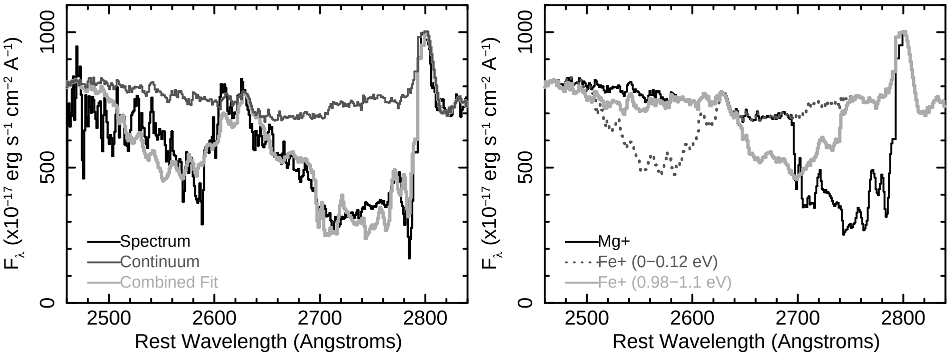

Figure 3. *Left:* The KPNO 4m spectrum of FBQS J1151+3822, showing the best fit model for a preliminary fit to the Mg ii/Fe ii feature using a model created with the He i*λ10830 absorption profile. *Right:* The three separate absorption components in the model (Lucy et al. in prep.).

log column densities of 15.0, 14.6 and 13.7 [cm^{-2}] for Mg ii, ground and low-excitation Fe ii, and high excitation Fe ii, respectively. For shallow features like the Fe ii features, Leighly et al. (2011) show that the spatially-averaged column is approximately equal to the column obtained from the apparent optical depth.

Our measurements of Mg ii and Fe ii place new strong constraints on the ionization parameter and therefore the column density. Fig. 4 shows *Cloudy* simulations of column densities of He i*, Mg$^+$ and Fe$^+$. We find that sufficient Mg ii is produced for $\log(U) \leq -1.4$. However, sufficient Fe$^+$ is attained only at $\log(U) \approx -1.55$, where He i* is ionization bounded (i.e., the He i* predicted in a semi-infinite slab is equal to the measured value). This is a consequence of the atomic properties of Mg and Fe. In the H ii region, Mg$^+$ and Fe$^+$ are produced by recombination. The +2→+3 ionization potential for Mg is high, 80.1 eV, which means that there is plenty of Mg^{+2}, and therefore Mg^{+1} in the H ii region, more than enough to create the observed broad absorption line. But the similar ionization potential for Fe is 30.7 eV, implying that iron is distributed among many ionization states in the H ii region. This means that a much higher column is needed to observe Fe ii compared with Mg ii. Therefore, the difference between LoBALs (objects with only Mg ii) and FeLoBALs (objects that also have Fe ii) may be simply a difference in column density along the line of sight.

The strongly-constrained ionization parameter provides strong constraints for the column density as well. For example, for log gas density $\log n = 6.5$ [cm^{-3}], *Cloudy* models for He i* and Fe ii match the measured values of those components where $\log(N_H) = 21.65$ [cm^{-2}]. Mg ii far exceeds the measured value at this column density, implying that the Mg ii line is saturated.

The value of $\log(n)$ is constrained to be between 5.0 and 7.5 by the lack of Balmer absorption and the presence of excited state Fe ii. If we assume that the outflow is accelerated by radiative line driving, Leighly et al. (2011) show that $\log(n) > 7.0$. This constrains $\log(N_H) = 21.7$ [cm^{-2}], the absorption-line gas radius of 12–21 pc, mass flux between 18 and 31 solar masses/yr, log kinetic luminosity between 44.2 and 44.45 [erg s^{-1}], and ratio of kinetic to bolometric luminosity to between 0.3 and 0.5%. Hopkins & Elvis (2010) postulate that a ratio of kinetic to bolometric luminosity as low

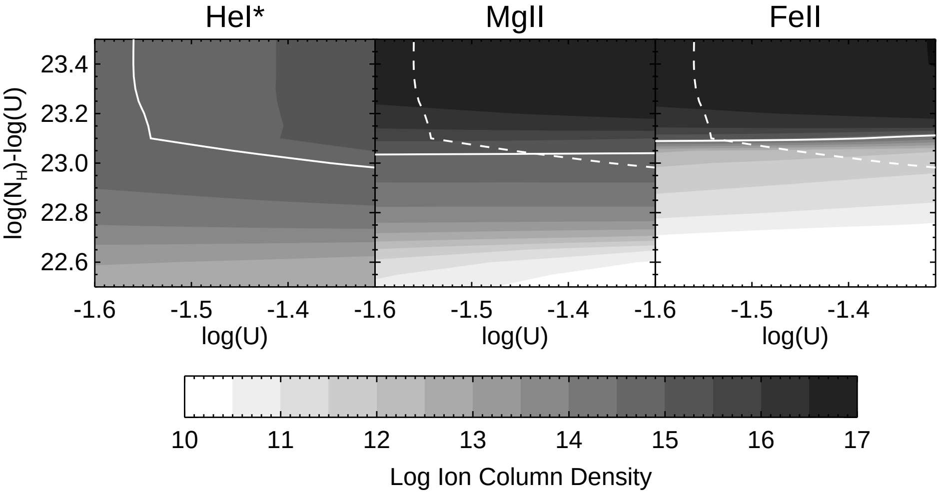

Figure 4. Column densities obtained using *Cloudy*. The solid white line shows the location in parameter space where the column density matches the measured value. The dashed line shows the He ɪ* average column on the other plots to guide the eye. While the He ɪ* and Mg ɪɪ values are consistent for $\log U \approx -1.4$, Fe ɪɪ requires $\log U = -1.55$, indicating that Mg ɪɪ is saturated.

as 0.5% may be sufficient to truncate star formation in AGN host galaxies. In that case, the outflow displayed in FBQS 1151+3822 may be just sufficient.

4. Summary and the Future

He ɪ* has been shown to be a powerful probe of high-column-density outflows in low redshift quasars. High column outflows are interesting because they may carry the most kinetic energy, and they potentially provide the greatest challenges to acceleration models. Low redshift objects are interesting since they provide potentially valuable targets for imaging. Furthermore, He ɪ* lines can be observed from the ground, which means that uniform samples can be identified and studied.

We have several followup projects in progress. Using IRTF, we observed a small sample of low-redshift quasars known to be BALQSOs. Some, like Mrk 231, have He ɪ*λ10830 absorption, and others do not. We identified 18 low-redshift quasars that have identifiable He ɪ*λ3889 in their SDSS spectra, and we have observed them using LBT Luci and/or Gemini GNIRS. This sample will allow a systematic investigation of covering fraction and column density as a function of other outflow parameters.

Acknowledgments. KML, ABL support: NSF AST-0707703, MD: AST-0604066.

References

Arav, N., Kaastra, J., Kriss, G. A., Korista, K. T., Gabel, J., & Proga, D. 2005, ApJ, 620, 665
Clegg, R. E. S. 1987, MNRAS, 229, 31P
Dunn, J. P., Bautista, M., Arav, N., Moe, M., Korista, K., Costantini, E., Benn, C., Ellison, S., & Edmonds, D. 2010, ApJ, 709, 611

Hamann, F. 1998, ApJ, 500, 798
Hamann, F., Barlow, T. A., Junkkarinen, V., & Burbidge, E. M. 1997, ApJ, 478, 80
Hopkins, P. F., & Elvis, M. 2010, MNRAS, 401, 7
Leighly, K. M., Dietrich, M., & Barber, S. 2011, ApJ, 728, 94